

Indirect processes in electron-impact ionization of Xe^{43+}

K. J. Reed and M. H. Chen

High Temperature Physics Division, Lawrence Livermore National Laboratory, Livermore, California 94550

D. L. Moores

Department of Physics and Astronomy, University College London, Gower Street, London WC1E 6BT, England

(Received 30 April 1990)

Relativistic-distorted-wave methods have been used to calculate electron-impact-ionization cross sections for Xe^{43+} . Cross sections were calculated for direct ionization of the $3s$ electron and the $n=2$ inner-shell electrons. Electron-impact-excitation cross sections were calculated for transitions from the $n=2$ subshells to the $n=3$ and 4 levels of the ion. Detailed Auger and radiative rates were calculated for the intermediate excited states and these were used to determine the excitation-autoionization and resonant-excitation double-autoionization contributions to the ionization cross section. Our results are in excellent agreement with reported experimental results for incident electron energies between 8 and 15 keV. Recent measurements using the electron-beam ion trap are in qualitative agreement with our results for energies between 4 and 8 keV.

Theoretical and experimental investigations of electron-impact ionization of sodiumlike ions have been reported in a number of papers during the past ten years. Earlier theoretical studies¹⁻⁵ of electron-impact ionization of lighter elements of this isoelectronic sequence predicted that excitation-autoionization cross sections are generally about 4 times the direct-ionization cross sections. Experimental results supported these predictions.^{6,7} In all of these earlier investigations, ions with atomic number less than 28 were studied. For those lighter elements it was observed that the effects of excitation autoionization increase with increasing atomic number, and this is understandable since direct-ionization cross sections decrease more rapidly with increasing atomic number than do excitation cross sections. However, until recently it has generally been assumed that excitation autoionization should be negligible in very-high- Z ions because of radiative decay of the intermediate levels. But a recent study of electron-impact ionization of Au^{68+} has indicated that significant excitation-autoionization effects persist for sodiumlike ions with atomic number as high as $Z=79$.⁸ It was found that the excitation-autoionization contribution in Au^{68+} was about 4 times the direct-ionization cross section at 1.5 times the $3s$ ionization threshold, which is about the same enhancement noted for the much lighter ions. In the case of Au^{68+} , this enhancement is the result of excitation to a few intermediate states that have large excitation cross sections and also large probabilities for Auger decay. It was also shown in Ref. 8 that it necessary to carry out detailed calculations of excitation cross sections and branching ratios for each intermediate state to obtain the contributions of these few levels since the contributions of these levels could be missed if averaging techniques are used in place of detailed calculations.

In addition to excitation autoionization, the indirect process of resonant-excitation double autoionization

(REDA) can contribute significantly to electron-impact-ionization cross sections for some ions. In a recent theoretical investigation of Fe^{15+} , careful consideration of REDA contributions shed light on a long-standing discrepancy between earlier theoretical and experimental results.⁹ In Au^{68+} the REDA contributions are significantly damped by radiative decay and contribute less than 5% of the total ionization cross section.⁸

In this paper we examine the effects of both REDA and excitation autoionization on the electron-impact-ionization cross sections for Xe^{43+} . We extend our calculations to incident electron energies up to 15 keV in order to compare our results with reported measurements.^{10,11} In the region of the excitation-autoionization thresholds, we compare our results with data recently obtained by Schneider *et al.*¹² using the electron-beam ion trap (EBIT).

Our calculational procedure has been described in detail elsewhere.^{8,9} Briefly, we carried out separate fully relativistic calculations of the direct-ionization cross sections, the cross sections for excitation to the intermediate autoionizing states, and the radiative and Auger rates for decay of the intermediate states.

The direct-ionization cross sections were calculated using a full partial-wave expansion method,¹³ in which the bound, incident, scattered, and ejected electron wave functions are computed in Dirac-Fock potentials.¹⁴ We calculated cross sections for direct ionization of the $2s$ and $2p$ inner-shell electrons as well as for the $3s$ electron of the Xe^{43+} ion.

A relativistic distorted wave method¹⁵ was used to compute the cross sections for exciting the $2s$ and $2p$ electrons to the $n=3$ and 4 subshells. Relativistic configuration-interaction (CI) wave functions for the target ion were generated using a Dirac-Fock atomic-structure code developed by Hagelstein and Jung.¹⁵ The $2s^2 2p^6 3l$, $2s^2 2p^5 3l n l'$, and $2s 2p^6 3l n l'$ ($n=3,4$) configu-

rations were included in the target description. We considered the following excitation-autoionization processes:

$$2s^2 2p^6 3s + e \rightarrow 2s^2 2p^5 3snl \quad (n=3,4) + e \rightarrow 2s^2 2p^6 + e + e, \quad (1)$$

$$2s^2 2p^6 3s + e \rightarrow 2s^2 2p^6 3sl \quad (n=3,4) + e \rightarrow 2s^2 2p^6 + e + e, \quad (2)$$

$$2s^2 2p^6 3s + e \rightarrow 2s^2 2p^5 3p^2 + e \rightarrow 2s^2 2p^6 + e + e. \quad (3)$$

The $2s^2 2p^5 3p^2$ intermediate states in Eq. (3) can be excited by configuration interaction.

We also include contributions due to the REDA process. This process is represented in Eq. (4):

$$2s^2 2p^6 3s + e \rightarrow 2s^2 2p^5 3snln'l' \rightarrow 2s^2 2p^5 3sn''l'' + e \rightarrow 2s^2 2p^6 + e + e. \quad (4)$$

Explicit calculations were performed for resonant states $2p^5 3s 4l 4l'$ and $2p^5 3s 3lnl'$ ($n=7-12$). An n^{-3} scaling law for Auger transition was used to extrapolate to $n=30$.

Since some of the intermediate excited states can decay radiatively as well as by autoionization, the excitation cross sections are multiplied by branching ratios in order to obtain the correct contribution to the ionization cross section. The branching ratios for single Auger emission B_i^A and sequential double Auger emission B_k^{DA} are given in Eqs. (5) and (6):

$$B_i^A = \sum_j A_{ij}^A / \left[\sum_m A_{im}^A + \sum_k A_{ik}^r \right] \quad (5)$$

and

$$B_k^{DA} = \sum_{k'} A_{kk'}^A \sum_f A_{k'f}^A / \left[\left(\sum_m A_{km}^A + \sum_n A_{kn}^r \right) \times \left(\sum_m A_{k'm}^A + \sum_n A_{k'n}^r \right) \right], \quad (6)$$

where A_{ij}^A and A_{ik}^r are the Auger transition from state i to j and radiative decay rate from state i to k , respectively.

The energy-averaged dielectronic capture cross section in cm^2 is obtained from the inverse Auger process by detailed balance:³

$$Q_k^{\text{cap}} = \frac{4.95 \times 10^{-30}}{\Delta E E_k} \frac{g_k}{2g_i} A_{ki}^A. \quad (7)$$

Here, ΔE and E_k are, respectively, the energy bin and Auger energy in eV; g_k and g_i are the statistical weights for the intermediate state k and the initial state i , respectively.

The detailed Auger and radiative rates required to calculate the branching ratios and capture cross sections were computed using the multiconfiguration Dirac-Fock (MCDF) model.¹⁶ The wave functions and energy levels for the excited states were calculated explicitly in inter-

mediate coupling, including configuration interaction within the same complex using the MCDF in the average-level scheme.¹⁷

Assuming that the direct and indirect ionization processes are independent, the total cross section Q_i is given by

$$Q_i = Q_d + \sum_i Q_i^{\text{ex}} B_i^A + \sum_k Q_k^{\text{cap}} B_k^{\text{DA}}, \quad (8)$$

where Q_d is the direct-ionization cross section; Q_i^{ex} and Q_k^{cap} are excitation and energy-averaged capture cross sections, respectively.

In Fig. 1 we show our computed results for incident electron energies between 4.2 and 5.6 keV. In this region, the direct-ionization cross section is a smooth and slowly varying function of incident electron energy and is shown by the dashed line in the figure. Above 4.2 keV the cross section begins to increase abruptly in a series of steps corresponding to excitation of $n=2$ electrons to autoionizing intermediate states as in processes (1), (2), and (3). The dotted curve is the sum of the direct-ionization cross section and the excitation cross sections.

The solid curve is the total ionization cross section with radiative decay taken into account. A branching ratio was computed for each intermediate state as in Eq. (5). Each excitation cross section was multiplied by a branching ratio and the resulting cross sections were added to the direct cross section.

The first large increase in the dotted curve starting around 4.38 keV is due to the combined effect of three transitions that are nearly degenerate. Radiative decay diminishes the contributions of these excitations and the resulting increase in the solid curve is relatively small. The next large increase near 4.41 keV is due to a single transition to the $2s^2 2p_{1/2}^2 2p_{3/2}^3 3s(2)3p_{3/2}$, $J=1/2$ state. (In this notation the number in parentheses represents the total angular momentum before coupling with the outer-

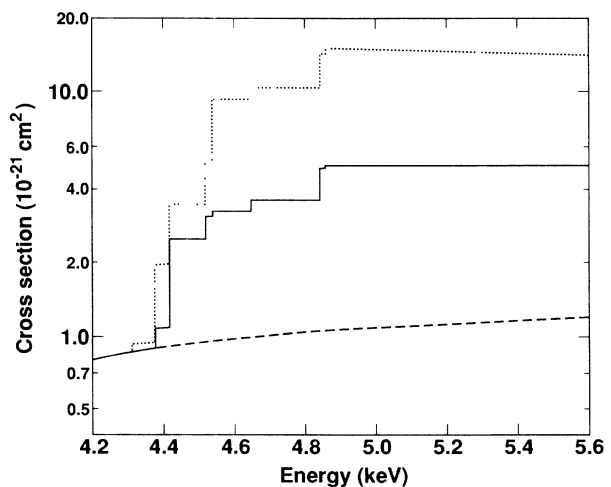


FIG. 1. Excitation autoionization in Xe^{43+} . Dashed curve, direct ionization cross section; dotted curve, total cross section with excitation autoionization but without radiative decay; solid curve, total ionization cross section with allowance for radiative decay.

most electron.) This transition has a large excitation cross section of $1.51 \times 10^{-21} \text{ cm}^2$ near threshold. It also has a very large branching ratio of 0.966, so that nearly every excitation to this level autoionizes and contributes to the ionization cross section.

The increase near 4.52 keV is the combined effect of the $2s^2 2p_{1/2}^2 2p_{3/2}^3 3s(1)3d_{5/2}$, $J=3/2$ transition and the transition to the $2s^2 2p_{1/2}^2 2p_{3/2}^4 3s^2$, $J=1/2$ state. Both transitions have moderately large excitation cross sections. But the $2s^2 2p_{1/2}^2 2p_{3/2}^3 3s(1)3d_{5/2}$, $J=3/2$ level, with a branching ratio of 0.06, can rapidly decay by strong dipole-allowed transitions. The $2s^2 2p_{1/2}^2 2p_{3/2}^4 3s^2$ level with a branching ratio of 0.40 accounts for the major part of the increase in the solid curve near this energy.

The largest excitation cross section is for the $2s^2 2p_{1/2}^2 2p_{3/2}^3 3s(2)3d_{5/2}$, $J=3/2$ state, which has a cross section of $2.75 \times 10^{-21} \text{ cm}^2$ near threshold. However, because of its small branching ratio of 0.03, this level contributes only slightly to the total ionization cross section. Most of the excitation cross sections are between 10^{-23} and 10^{-22} cm^2 , but a few are as small as 10^{-26} cm^2 . The branching ratios range from 10^{-4} to 1.0.

At 5.6 keV (which is about 1.5 times the $3s$ ionization threshold), the excitation autoionization processes enhance the direct-ionization cross section by about a factor of 4. This is approximately the same enhancement noted for Au^{68+} (Ref. 8) and Fe^{15+} (Ref. 9), as well as for the lighter sodiumlike ions studied in earlier investigations. Although the overall enhancement is roughly the same, the relative contribution from various intermediate states differs among the ions for which detailed calculations have been carried out. For example, the $2p_{1/2}^2 2p_{3/2}^4 3s^2$ state makes a fairly significant contribution to the total ionization cross section in Xe^{43+} , while the contribution of this level is negligible in Au^{68+} and Fe^{15+} . This stems from the differences in the effects of configuration interaction in these three ions. In Xe^{43+} the $2p_{1/2}^2 2p_{3/2}^4 3s^2$ has a fairly large component (i.e., 0.2005) from the $2p_{1/2}^2 2p_{3/2}^3 3s 3d_{5/2}$, $J=1/2$ state. This $2p_{1/2}^2 2p_{3/2}^3 3s 3d_{5/2}$, $J=1/2$ level has one of the largest excitation cross sections, and the mixing with this state increases the cross section for exciting the $2p_{1/2}^2 2p_{3/2}^4 3s^2$ transition in Xe^{43+} . On the other hand, this mixing coefficient is relatively small for these two states in Fe^{15+} (i.e., 0.0335), and in Au^{68+} (i.e., -0.0145). While configuration interaction plays a relatively minor role in excitation autoionization for Au^{68+} , CI effects are considerably more important in Xe^{43+} . The $2s^2 2p^5 3p^2$ intermediate states, which are excited by configuration interaction, contribute only 5% of the total cross section for Au^{68+} .⁸ In Xe^{43+} these states contribute almost 20% to the total ionization cross section. Nevertheless, the dominant contribution to excitation-autoionization enhancement of the ionization cross section arises from the $2p_{1/2}^2 2p_{3/2}^3 3s(2)3p_{3/2}$, $J=1/2$ intermediate state in each of the three ions.

Figure 2 shows the contribution due to REDA, which is manifested as a series of narrow resonances. In the figure each REDA resonance is convoluted with a Gaussian 5 eV in width. The resonances above 4.6 keV are due to $2p^5 3s 3l n l$ states. Those resonances below 4.6 keV are

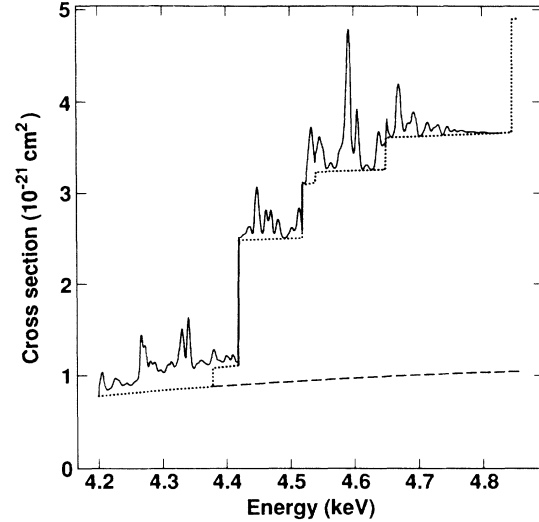
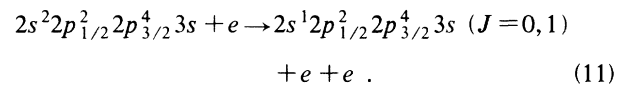
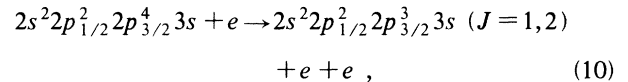
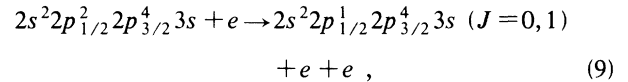


FIG. 2. Resonant-excitation double autoionization in Xe^{43+} . Dashed curve, direct ionization; dotted curve, cross section with excitation autoionization (radiative decay included); solid curve, total cross section with REDA.

due to the $2p^5 3s 3l n l$ states and the $2p^5 4l 4l'$ states as well. Overall, the REDA contribution is about 20% of the total ionization cross section.

Above 7.5 keV direct ionization of the electrons in the $n=2$ subshells begins to contribute. In addition to direct ionization of the $3s$ electron, we calculated cross sections for the following direct-ionization processes:



The threshold for processes (9), (10), and (11) are 7.56, 7.89, and 8.20 keV, respectively. The thresholds obtained for the different J values were nearly identical in each case. The contributions from processes (9), (10), and (11) are shown in Fig. 3 along with the cross section for direct ionization of the $3s$ electron. The $2p$ inner-shell ionization cross section increases rapidly from threshold and is greater than the $3s$ ionization cross section above 10 keV. The contribution of $2s$ ionization is small, but not negligible. It is clear that neglect of these inner-shell ionizations would result in serious underestimation of the direct-ionization cross section above 8 keV.

In Fig. 4 we compare our theoretical results to cross sections obtained in two different experiments. In 1982, measurements of electron-impact-ionization cross sections for xenon ions were reported by Donets.¹¹ These measurements were made using an electron-beam ion method (EBIM) and included ionization cross sections for

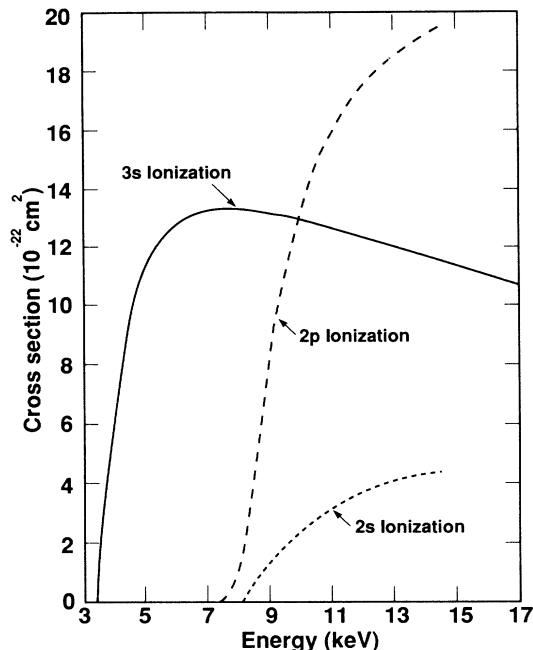


FIG. 3. Contributions to direct ionization of Xe^{43+} . Solid curve, cross sections for 3s ionization; dashed curve, sum of cross sections for $2p_{1/2}$ and $2p_{3/2}$ inner-shell ionization; dotted curve, cross section for 2s inner-shell ionization.

Xe^{43+} above 8 keV. In 1989, Andrianmonje *et al.*¹⁰ reported electron-impact-ionization cross sections deduced from measurements made on 27-MeV/ μ Xe^{35+} beams channeled through a thin silicon crystal. For Xe^{43+} their results were slightly higher than the results reported by Donets. In Fig. 4 it can be seen that our calculated cross sections (solid curve) are in excellent agreement with the measurements reported by Donets (open circles) for energies between 8 and 15 keV.

The solid circles in Fig. 4 represent data obtained in recent measurements using the EBIT.¹² The measurements are in good qualitative agreement with our calculated ionization cross sections. Although resolution in the EBIT experiments is not sufficient to show the step structure, the measurements clearly indicate a steep rise in the ionization cross section in the region where the excitation-autoionization processes contribute to our

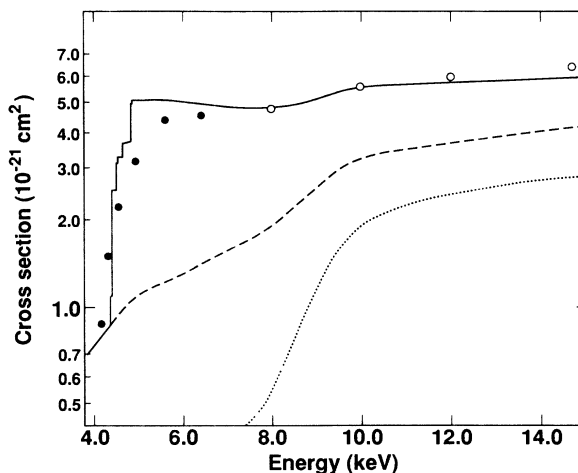


FIG. 4. Cross sections for electron impact ionization of Xe^{43+} . Dotted curve, sum of ionization cross sections for $n=2$ inner-shell electrons; dashed curve, total direct ionization cross section; solid curve, computed total ionization cross section; open circles, measurements from Ref. 11; solid circles, measurements from Ref. 12.

computed cross sections.

In conclusion, we have calculated direct, REDA, and excitation-autoionization contributions to the cross sections for electron-impact ionization of Xe^{43+} . The excitation-autoionization contribution enhances the direct-ionization cross section by a factor of 4 at 1.5 times the ionization threshold and the REDA contribution adds about 20% to the total cross section in the threshold region. Our results are in excellent agreement with experimental results for incident electron energies above 8 keV, and there is good qualitative agreement with recent results obtained in EBIT experiments in the 4–8-keV range.

We thank D. Schneider for stimulating discussions. We also thank I. P. Grant and F. A. Parpia for access to the unpublished code GRASP2 and for valuable assistance in using it. This work was performed under the auspices of the U.S. Department of Energy by the Lawrence Livermore National Laboratory under Contract No. W-7405-ENG-48.

¹D. L. Moores and H. Nussbauer, *J. Phys. B* **3**, 6 (1970).

²R. D. Cowan and J. B. Mann, *Astrophys. J.* **232**, 940 (1979).

³K. T. LaGattuta and Y. Hahn, *Phys. Rev. A* **24**, 2273 (1981).

⁴D. C. Griffin, C. Bottcher, and M. S. Pindzola, *Phys. Rev. A* **25**, 154 (1982); **36**, 3642 (1987).

⁵R. J. W. Henry and A. Z. Msezane, *Phys. Rev. A* **26**, 2545 (1982).

⁶D. H. Crandall *et al.*, *Phys. Rev. A* **25**, 143 (1982).

⁷D. C. Gregory, L. J. Wong, F. W. Meyer, and K. Penn, *Phys. Rev. A* **35**, 3256 (1987).

⁸K. J. Reed, M. H. Chen, and D. L. Moores, *Phys. Rev. A* **41**, 550 (1990).

⁹M. H. Chen, K. J. Reed, and D. L. Moores, *Phys. Rev. Lett.* **64**, 1350 (1990).

¹⁰S. Andrianmonje *et al.*, *Phys. Rev. Lett.* **63**, 1930 (1989).

¹¹E. D. Donets, *Phys. Scr.* **T3**, 11 (1983).

¹²D. Schneider *et al.*, *Phys. Rev. A* (to be published).

¹³D. L. Moores and M. S. Pindzola (unpublished).

¹⁴K. G. Dayall, I. P. Grant, C. T. Johnson, and E. P. Plummer, *Comput. Phys. Commun.* **55**, 425 (1989).

¹⁵P. L. Hagelstein and R. K. Jung, *At. Data Nucl. Data Tables* **37**, 17 (1987).

¹⁶M. H. Chen, *Phys. Rev. A* **31**, 1449 (1985).

¹⁷I. P. Grant *et al.*, *Comput. Phys. Commun.* **21**, 207 (1980).